



Early result from the inter-sensor comparison of Himawari-8

Advanced Himawari Imager with the Visible Infrared Imaging Radiometer Suite

Mike Chu^{1,2}, Xiangqian Wu² and Fangfang Yu^{1,2}

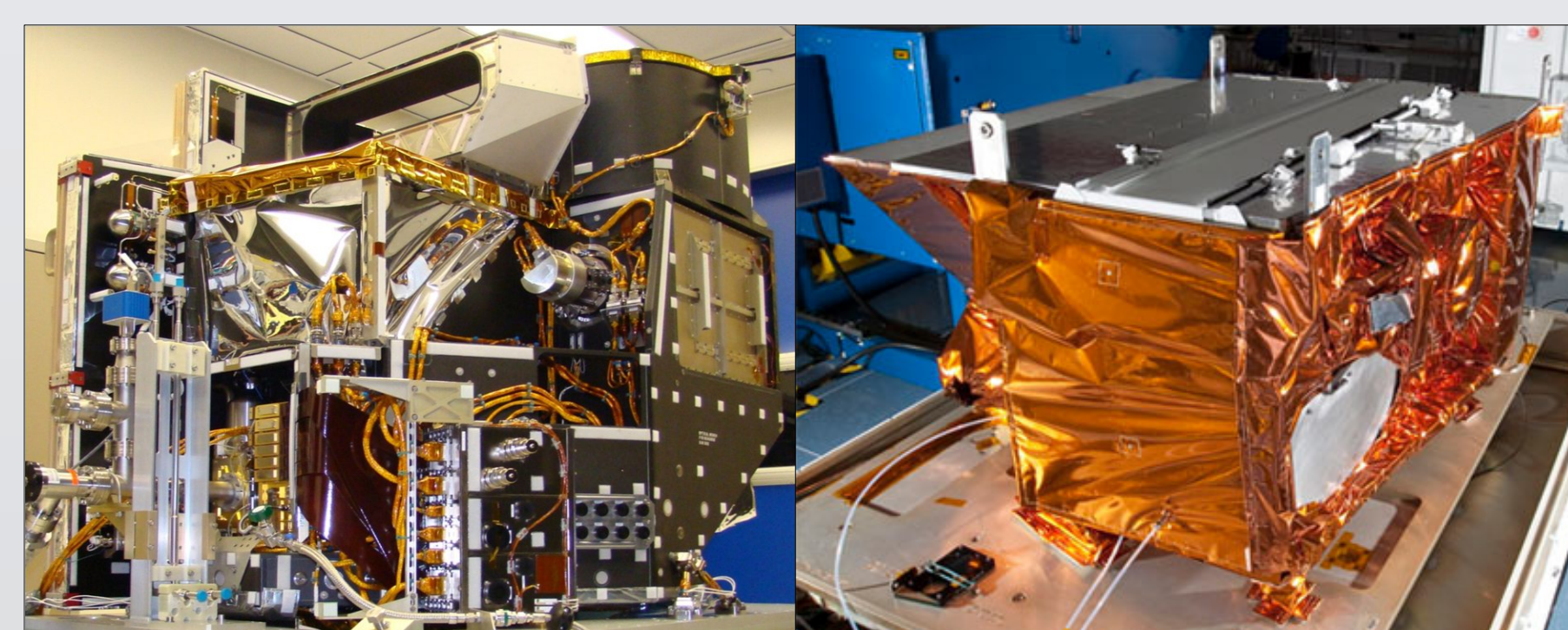
1 – ERT, 2 – NOAA/NESDIS/STAR



The Sensors

The Advanced Himawari Imager (AHI) is the next-generation geostationary instrument for the Japanese Meteorological Agency (JMA) to continue on the legacy of the weather monitoring and forecast in the East Asian and Western Pacific regions. The sensor is on board the Himawari-8 satellite successfully launched on October 7th, 2015. In a collaborative effort with the JMA, the GOES-R Calibration Working Group (CWG) has been working to study the performance of AHI and the applicable risk-mitigation for GOES-R Advanced Baseline Imager (ABI).

An assessment of the radiometric performance of the 6 AHI solar bands is carried out via an inter-sensor comparison with the Visible Infrared Imaging Radiometer Suite (VIIRS) on board the Suomi National Polar-orbiting Partnership (SNPP) satellite utilizing deep convective clouds (DCC) near the AHI sub-satellite point (SSP). The two instruments are shown in Figure 1.



JMA Himawari-8 AHI / NOAA S-NPP VIIRS

Figure 1: The left panel displays AHI sensor unit and the right panel displays the VIIRS sensor unit. Photos credit: JMA/MS&C & NOAA/NESDIS

AHI-VIIRS Match

The AHI-VIIRS orbit crossing on Feb 7th, 2015 shown in Figure 2 typifies the expected match. The central cross marks the AHI geostationary SSP at 140° east longitude and 0° latitude over an AHI B13 (10.35μm) UTC 0230 imagery. VIIRS polar-orbiting ground tracks are illustrated in squares. The spatial domain of interest for our analysis is ±15 degrees latitude and ±30 degrees of AHI SSP bounded by the dashed outlines.

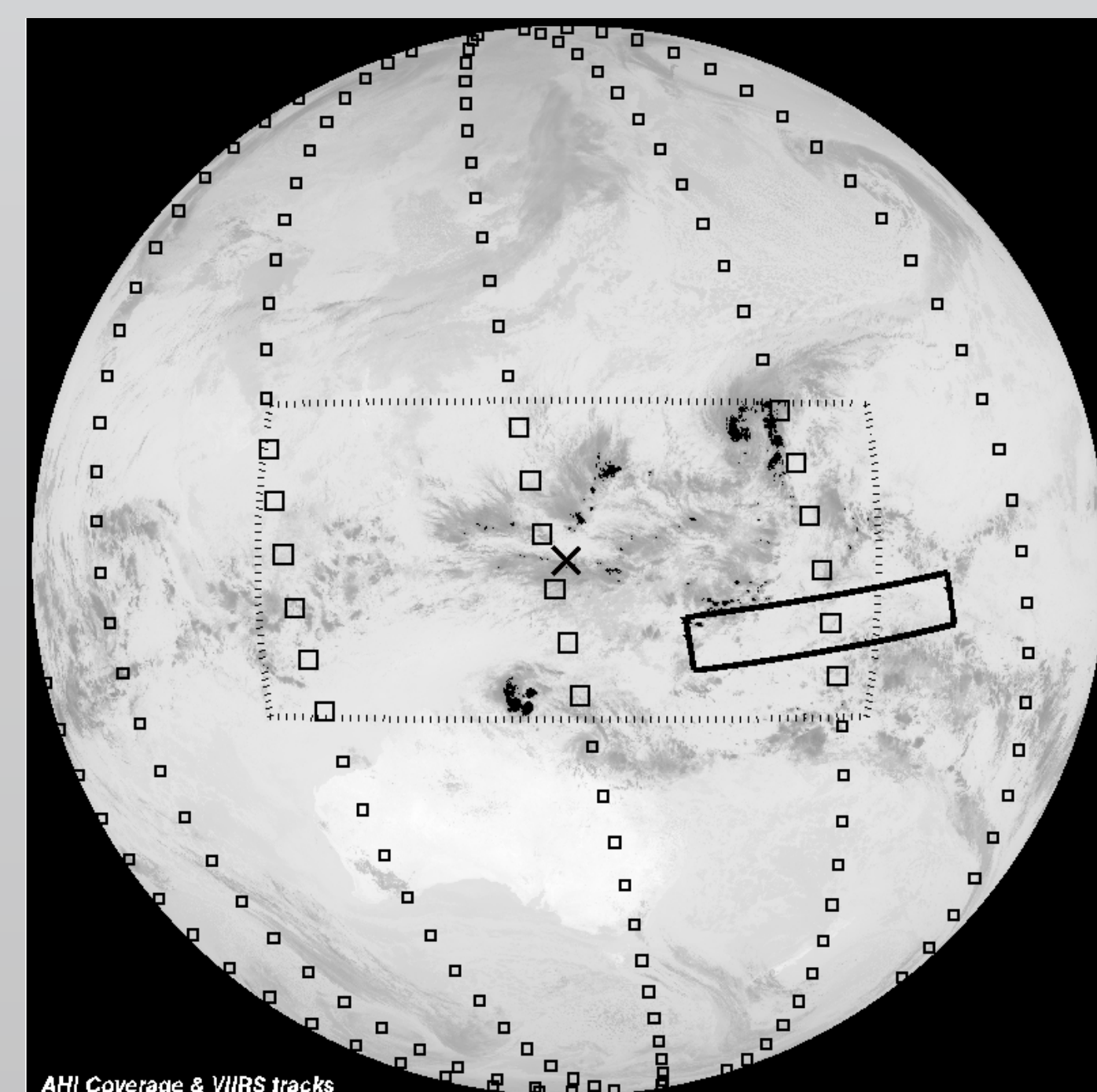


Figure 2: An AHI B13 image is superimposed with the AHI SSP marked by the central cross, VIIRS ground tracks in squares, a VIIRS swath in solid outlines, and the spatial domain for the comparison analysis in dashed outlines.

AHI-VIIRS Solar Bands and Spectral Response Comparison

The 6 AHI solar bands in the vis and near-infrared (VNIR) spectral region have well-matched corresponding VIIRS moderate bands. The wavelengths and the resolution of the 6 matching AHI-VIIRS band pairs are listed in Table 1 and the spectral response functions (SRF) are plotted in Figure 3.

AHI			VIIRS		
Band Designation	Wavelength (μm)	Resolution (km)	Band Designation	Wavelength (μm)	Resolution (km)
1	0.47	1.0	M3	0.48	0.75
2	0.51	1.0	M3	0.48	0.75
3	0.64	0.5	M5	0.67	0.75
4	0.86	1.0	M7	0.87	0.75
5	1.60	2.0	M10	1.61	0.75
6	2.25	2.0	M11	2.25	0.75

Table 1: The wavelengths and the resolutions of the 6 AHI VNIR solar bands and the matching VIIRS moderate bands

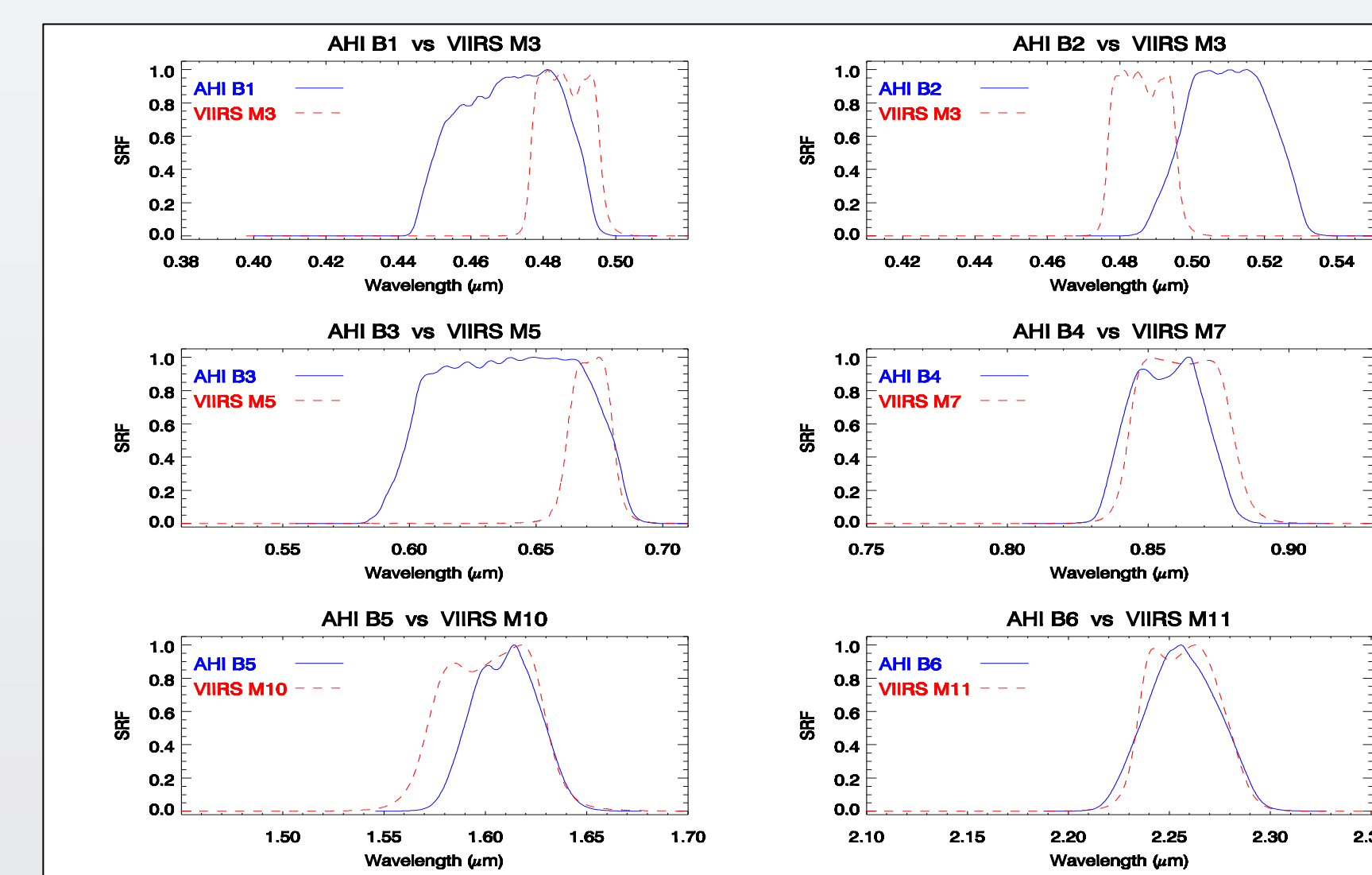


Figure 3: The spectral response functions of the 6 AHI solar bands and the matching VIIRS bands.

AHI Geolocation Accuracy, Co-Registration and Diurnal Variation

The early AHI dataset from Feb 7th, 2015 through Feb 13th, 2015 are image registration and navigation (INR) and co-registration enabled. We examine the dataset for remaining inaccuracy. Figure 4 displays a landmark test, with the supposed central location of an “Unnamed Reef” indicated by a black pixel, showing VIIRS M3 imagery to be accurate but that AHI B1 radiance imagery deviates by 1 pixel (~1km) at around UTC 05:30 on Feb 7th, 2015. Figure 5 illustrates the co-registration between AHI B13 and B1 to be accurate at the sub-pixel level. Figure 6 shows diurnal variation on Feb 7th showing 1 to 3km differences using the same landmark as one in Figure 4. The diurnal effect also shows in B2 and B3, and persists for all 7 days.

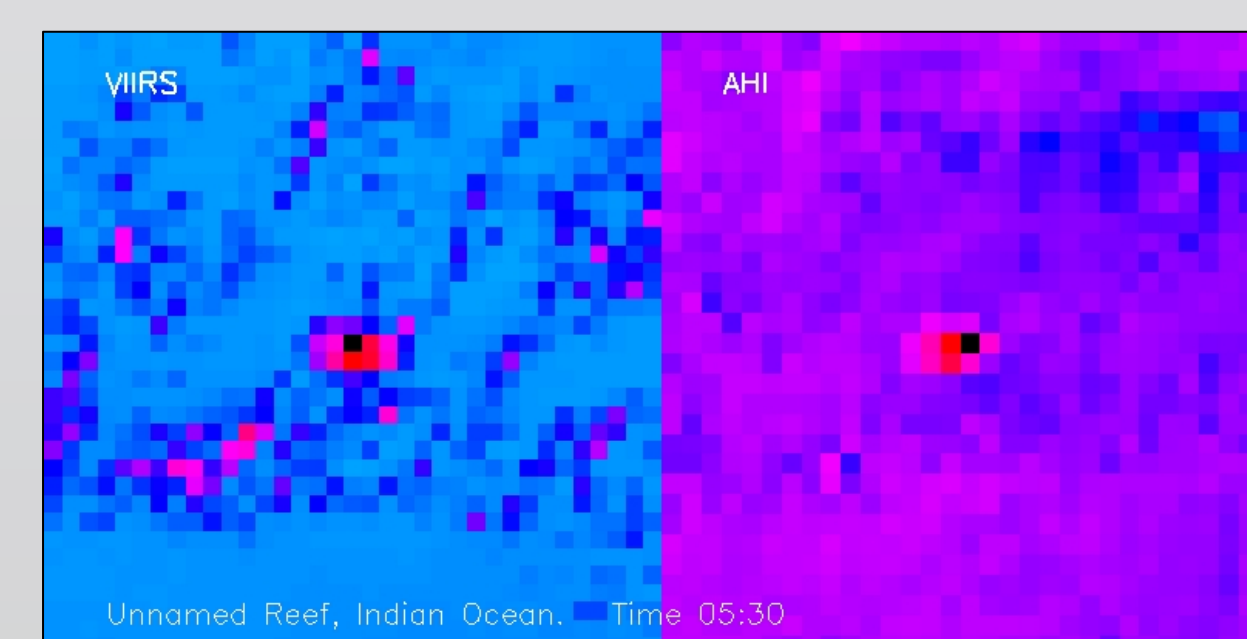


Figure 4: The navigation accuracy is illustrated for VIIRS M3 imagery on the left panel versus AHI B1 imagery on the right panel using a landmark at 12.511 south latitude and 123.557 east longitude. The black pixel marks where landmark center should be.

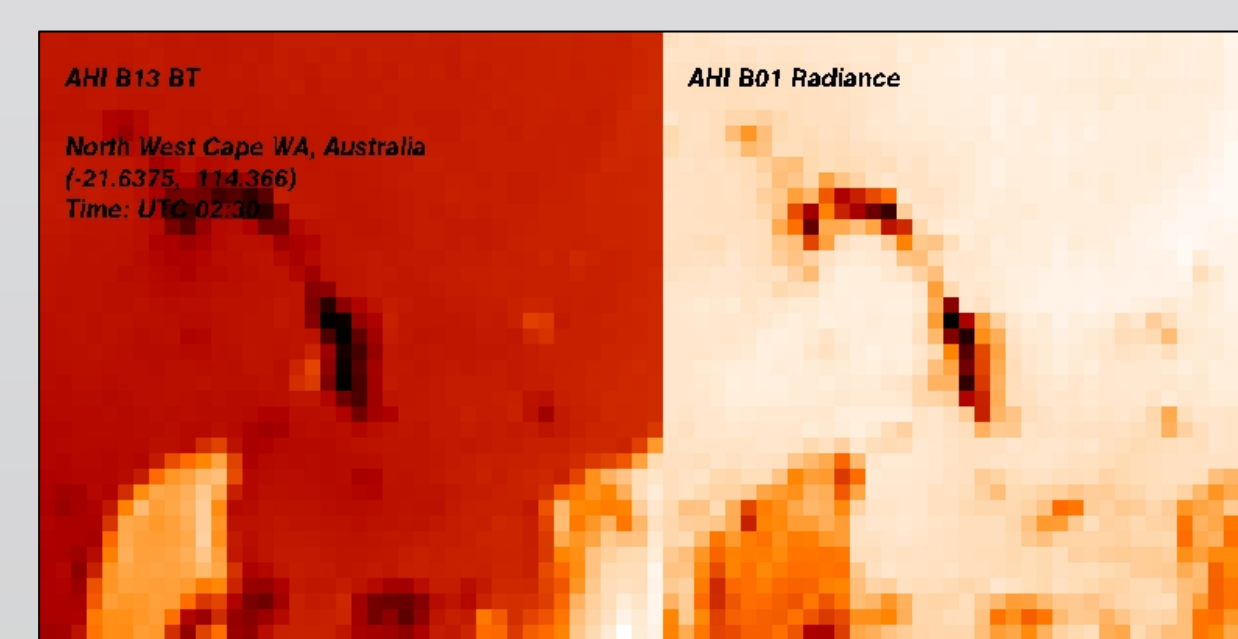


Figure 5: Co-registration between AHI B13 and B1 is established at the sub-pixel level using a land-ocean boundary.

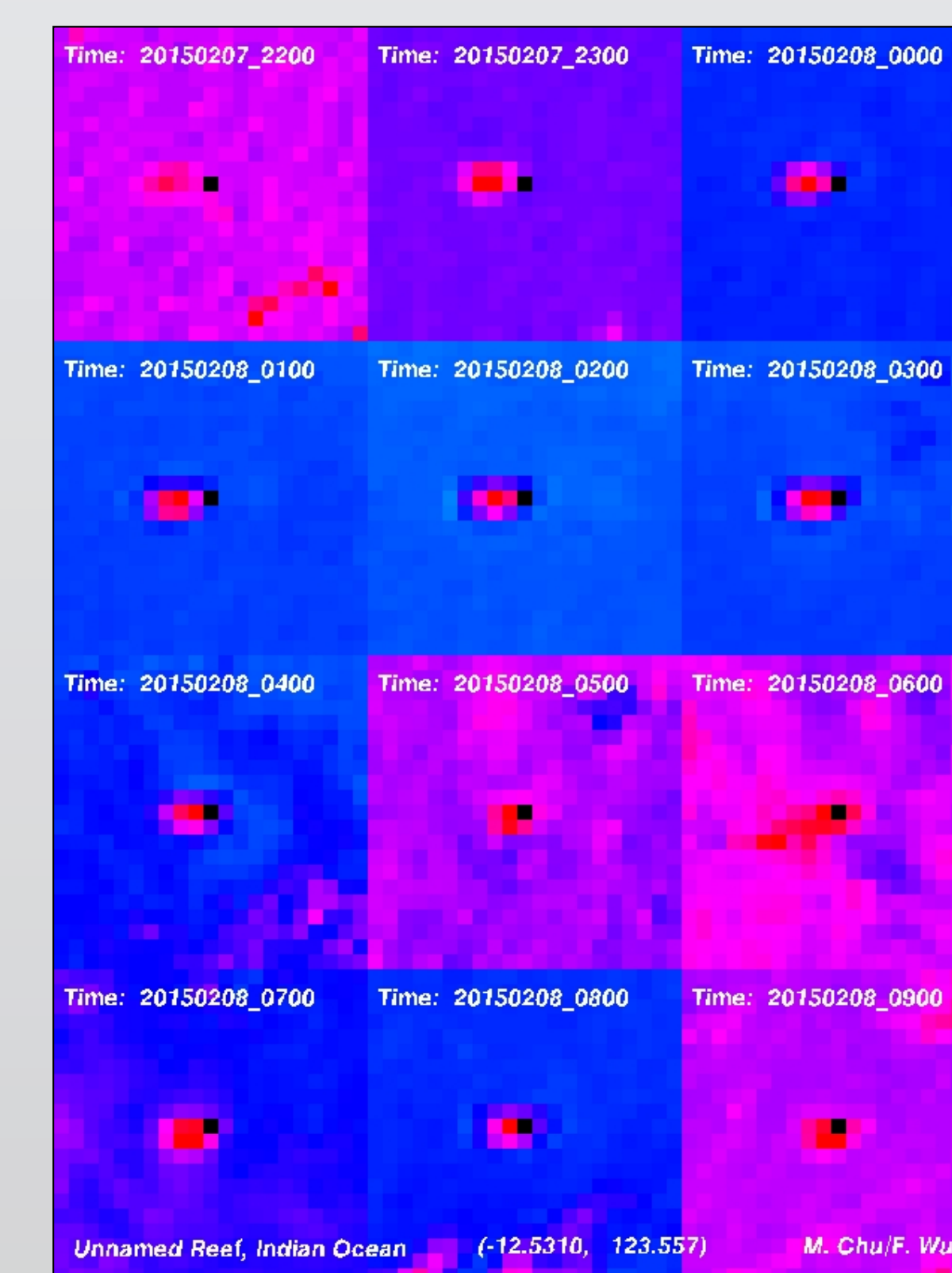


Figure 6: An imagery time-series showing diurnal variation in the navigation of AHI B1 imagery on Feb 7th, 2015.

Deep Convective Clouds Analysis

Deep convective clouds (DCC) being solar-diffuser-like objects with near-Lambertian reflectance property and abundant in the equatorial band are well-suited for this inter-sensor comparison analysis to examine the radiometric performance of AHI solar bands in the early going. The DCC pixels are identified by AHI B13 (10.35μm) using the brightness temperature (BT) threshold $BT < 205\text{ K}$ with a 1K uniformity condition $\sigma_{BT} < 1\text{ K}$ [1]. In Figure 2, DCC are accentuated as dark pixels and only those in the spatial domain within dashed outline are used. An additional threshold limiting the viewing angle difference between the two sensors is selected to be 10 degrees to balance between sample size and statistical quality.

A ratio of radiance is calculated for each AHI-VIIRS matching band pair and for each corresponding AHI B13 DCC pixel. The spectral band adjustment factor (SBAF) accounting for SRF difference is also applied to each ratio:

$$r = sbaf * \frac{Rad_{Ahi}}{Rad_{VIIRS}}$$

The SBAF for the first 4 matching band pairs are directly obtained from the web-calculator based on SCHIAMACHY visible hyper-spectral data [2] and the SBAF for the bottom 2 matching band pairs, not available from the SCHIAMACHY web-tool, is estimated and expected to be accurate within 1%.

AHI-VIIRS Radiance Comparison Result

The AHI data used in the comparison analysis are first corrected for the remaining INR diurnal variation. The daily result from the 3 matching VIIRS tracks as illustrated in Figure 2, typically within UTC 0150 and UTC 0630, is combined into a single statistic. The 7-day trend for the 6 AHI solar bands is shown in Figure 7, with star symbols and vertical bars indicating the daily mean and standard deviation. This preliminary result suggests that B1 (0.47μm) and the B4 (0.86μm) are accurate while B2 (0.51 μm) and (1.61 μm) are marginally acceptable within uncertainty. However, B3 (0.64μm) and B6 (2.26μm) result suggests a dark bias by as much as 10%.

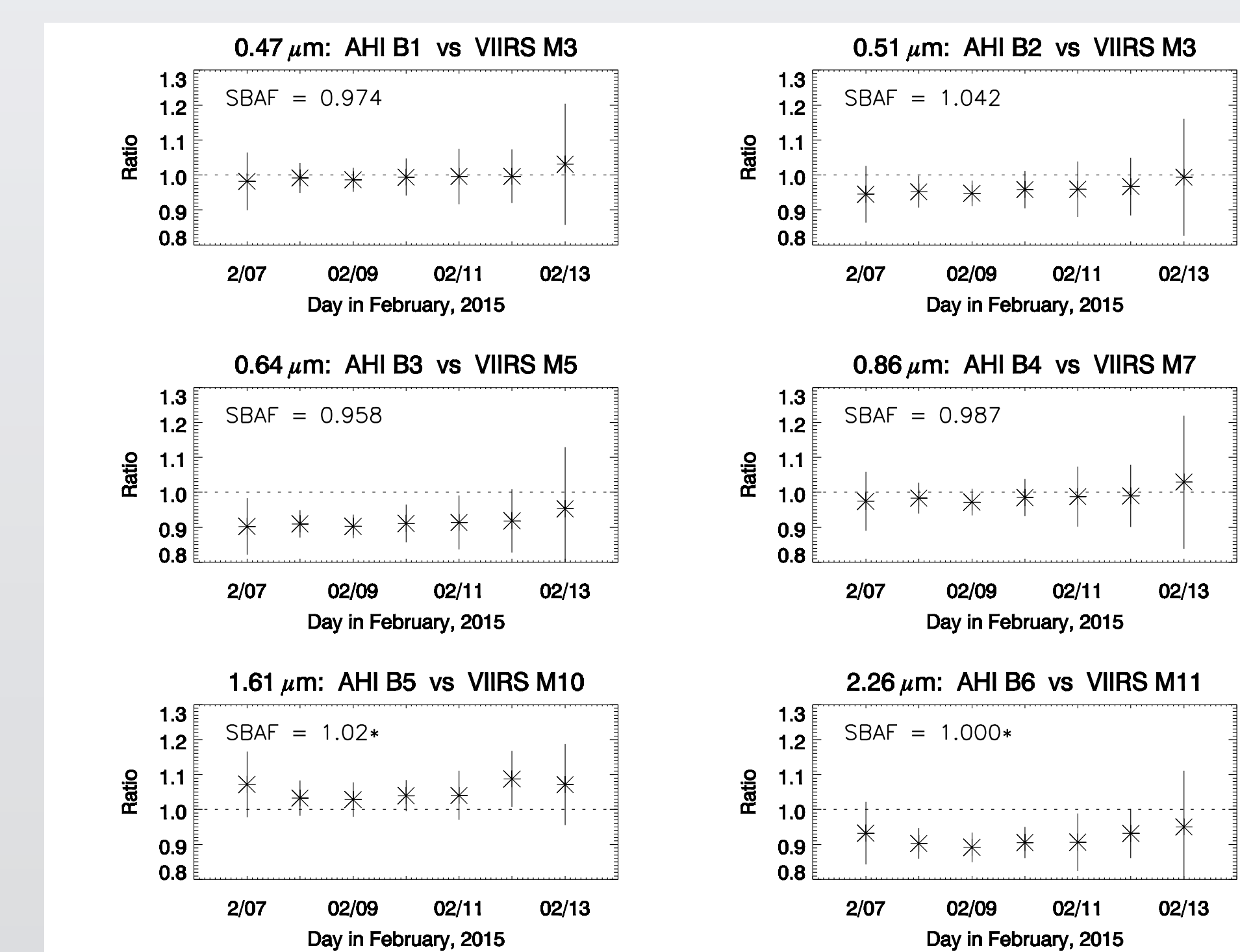


Figure 7: AHI-VIIRS radiance comparison trend of the 6 AHI solar bands in an early 7-day period.

Summary

A preliminary assessment of the radiometric performance of the AHI solar bands has been carried out using DCC and inter-sensor comparison with VIIRS. The result reveals a possible dark bias for the AHI 0.64μm and the 2.26μm bands requiring further investigation. The comparison analysis using DCC and VIIRS has been demonstrated to be useful for the early performance assessment of AHI solar bands and can be applied for GOES-R ABI.

Acknowledgements

The CWG would like to acknowledge valuable contributions from the following:

- Japanese Meteorological Agency
- Yi Song and Walter Wolf's team

References

- [1] Doelling, D.R.; Daniel, M.; Benjamin, R.S.; Rajendra, B.; Arun, G. The characterization of deep convective clouds as an invariant calibration target and as a visible calibration technique. *IEEE Trans. Geosci. Remote Sens.* **2013**, *51*, 1147-1159.
- [2] Scarino, B., D. R. Doelling, P. Minnis, A. Gopalan, T. Chee, R. Bhatt, C. Lukashin, and C. O. Haney, "A Web-based Tool for Calculating Spectral Band Difference Adjustment Factors Derived from SCHIAMACHY Hyper-spectral Data," Submitted to *IEEE Trans. Geosci. Remote Sens.*, 2014.